



A novel approach towards solvent-free epoxidation of cyclohexene by Ti(IV)–Schiff base complex–intercalated LDH using H₂O₂ as oxidant

K.M. Parida*, Mitarani Sahoo, Sudarshan Singha

C & MC Department, Institute of Minerals & Materials Technology, Bhubaneswar 751 013, Orissa, India

ARTICLE INFO

Article history:

Received 1 August 2010
Revised 9 September 2010
Accepted 10 September 2010
Available online 15 October 2010

Keywords:

Layered double hydroxide
Ti(IV)-complex
Solvent free
Epoxidation reaction
Intercalation

ABSTRACT

A novel heterogeneous catalyst has been developed by immobilizing Ti(IV)–Schiff base complex in Zn–Al/LDH by an ion-exchange method. Powder X-ray diffraction, Fourier transform infrared spectroscopy, diffuse reflectance UV–Visible spectroscopy, N₂-adsorption and thermal studies confirm the successful intercalation of the Ti-complex within the LDH structure. The supported catalyst shows an excellent catalytic activity in cyclohexene epoxidation reaction. In this paper, we report an environmentally benign reaction pathway in a solvent-free condition, taking H₂O₂ as oxidant. As high as 95% conversion of cyclohexene took place at 70 °C in 6 h. The heterogeneous catalyst can be recovered easily and reused multiple times without significant loss in catalytic activity and selectivity, which is a better green alternative for practical applications.

© 2010 Elsevier Inc. All rights reserved.

1. Introduction

One of the challenges facing chemists this century is to develop new transformations that are not only efficient, selective and high-yielding but are also environmentally benign [1,2]. The utilization of nontoxic chemicals, renewable materials and solvent-free conditions are the key issues in the green synthetic strategy. Solvent-free methods are of great interest in order to replace classical procedures making them profitable, cleaner, safer and operationally easier. Hydrogen peroxide is probably the preferred terminal oxidant after dioxygen due to environmental and economic considerations [3–6]. Indeed in certain circumstances, it is better than oxygen insofar as O₂/organic mixtures may sometimes be spontaneously ignited. So, epoxidation systems that use hydrogen peroxide as oxidant in a solvent-free condition in conjunction with recyclable and reusable heterogeneous catalysts are potentially viable for large-scale production.

The epoxidation of alkenes by the electrophilic addition of oxygen to a carbon–carbon double bond remains one of the most significant challenges in synthetic chemistry. The formed epoxides are the building block intermediates that can be converted to a variety of products [7,8]. The titanium(IV)-catalyzed reactions with a variety of different alkenes ranging from low molecular weight alkenes to large molecules are well known [4]. Titanium(IV) alkoxides catalyze the epoxidation of a variety of alkenes with an alkyl

hydroperoxide as the oxygen donor [9–14]. Propene can be efficiently epoxidized using hydrogen peroxide in an activated form of oxygen using the titanium silicalite TS-1 as catalyst [15]. But the reactions are relatively slow, and formation of by-products by the addition of tert. butyl hydroperoxide radical to the substrate is often observed [12]. These problems have been overcome by the development of a heterogeneous titanium catalyst [13].

Insertion of organic or organometallic species into inorganic solids offers an attractive route to nanohybrids in which complementary properties of the two components are expressed in a single material. Layered solids in which guest species can access interlamellar space via the intercalation process provide some of the best-studied examples of such systems [16]. Layered double hydroxides (LDH), also known as anionic clay, constitute a class of host–guest materials that have gained great attention recently. LDHs are brucite-like solids that are constituted by two metals typically having 2 + (M^{II}) and 3 + (M^{III}) oxidation states, octahedrally surrounded by oxo bridges and hydroxyl groups. The structure is organized forming layers that bear an excess of positive charge equivalent to the number of trivalent metals. This excess of positive charge requires the presence of charge compensating anions that are located in the interlayer spaces [17–22]. Sandra Gago et al. have reported immobilization of oxomolybdenum species in a LDH pillared by 2,2'-Bipyridine-5,5'-dicarboxylate anions for liquid-phase epoxidation of cis-cyclooctene, 1-octene and trans-2-octene using tert-butyl hydroperoxide as oxygen source [23]. LDH containing metal complexes of chelating ligands namely NTA (nitriloacetate) and EDTA (ethylenediamine tetraacetate) have also been prepared either by direct intercalation of metal

* Corresponding author. Fax: +91 674 258 1637.

E-mail address: paridakulamani@yahoo.com (K.M. Parida).

complexes or indirectly by forming metal complexes between the host layers following intercalation of the ligands [24].

In the present work, we describe a new protocol for immobilization of Ti(IV)-complex in the interlayer of LDH by replacing the interlayer gallery anions in an ion-exchange method. The heterogeneous Ti-complex so formed is found to be an excellent catalyst for epoxidation of cyclohexene in a solvent-free condition using H_2O_2 as oxidant.

2. Experimental

2.1. Materials

3-Amino-2-pyrazine carboxylic acid, 2-pyridine carboxaldehyde, titanium tetra-isopropoxide (Aldrich), $\text{Zn}(\text{NO}_3)_2 \cdot 6\text{H}_2\text{O}$ and $\text{Al}(\text{NO}_3)_3 \cdot 9\text{H}_2\text{O}$ (CDS) were used without further purification. Ethanol was dried using molecular sieve 5A prior to its use in the reaction.

2.2. Preparation of the catalysts

2.2.1. Preparation of LDH

The layered double hydroxide containing Zn:Al molar ratio 2:1 was prepared by the co-precipitation method at a constant pH of 11 [25]. The synthesis was carried out by dropwise addition of mixed metal nitrate solution [$\text{Zn}(\text{NO}_3)_2 \cdot 6\text{H}_2\text{O}$ (0.133 M) and $\text{Al}(\text{NO}_3)_3 \cdot 9\text{H}_2\text{O}$ (0.066 M)] to 2 M NaOH solution taken in a flask containing 100 ml of deionized water under magnetic stirring, and nitrogen atmosphere was maintained throughout the addition. The resulting slurry was kept stirring for 1 h at room temperature. Then, it was filtered, washed thoroughly with deionized water till the washings were neutral to litmus and dried at 100 °C overnight [26,27]. Elemental analysis showed the following composition. Found/calcd (%). For $\text{Zn}_{0.68}\text{Al}_{0.32}(\text{OH})_2(\text{NO}_3)_{0.32} \cdot 0.38 \text{H}_2\text{O}$ (Zn, Al-LDH- NO_3): Zn, 38.87/39.07; Al, 7.53/7.63; N, 3.86/3.93; H, 2.19/2.26. IR (KBr) 3450, 1620, 1384, 675, 445 cm^{-1} .

2.2.2. Synthesis of the metal complex

3-Amino-2-pyrazine carboxylic acid treated with Na_2CO_3 in ethanolic medium produces the sodium salt of 3-amino-2-pyrazine carboxylic acid. In 30 ml of ethanol, 10 mmol of sodium salt of 3-amino-2-pyrazine carboxylic acid was refluxed with 10 mmol of 2-pyridine carboxaldehyde. The whole mixture was kept on water bath at 60 °C for 2 h to produce the Schiff base ligand. Ti-complex was formed by refluxing 0.456 g (1.8 mmol) of sodium salt of Schiff base ligand and 0.29 ml (1 mmol) of titanium tetra-isopropoxide ($\text{C}_{12}\text{H}_{28}\text{O}_4\text{Ti}$) in ethanolic medium at 60 °C for 2 h. The final product was filtered, washed several times with ethanol to get rid of nonreacted ligand and recrystallized from diethyl ether. Finally, the metal complex was dried in vacuum and kept in a desiccator. Anal. Found/calcd (%). For ligand: C, 52.43/52.8; H, 2.57/2.8; N, 21.9/22.4. For Ti-complex: C, 47.98/48.17; H, 2.32/2.55; N, 20.02/20.43. IR (KBr) 3300, 1725, 1640 cm^{-1} . For Schiff base ligand: ^1H NMR (CDCl_3 , room temp., 200 MHz): δ = (7.15, t), (7.63, t), (7.7, d), (8.41, d), (8.59, s), (8.86, d), (8.71, d). ^{13}C CP MAS NMR (100.62 MHz, CDCl_3): δ = 130.1, 130.9, 131.4, 133.9, 134.1, 134.7, 138.7, 139.0, 148.2, 167.0, 167.7. For Ti-complex: ^1H NMR (CDCl_3 , room temp., 200 MHz): δ = (7.18, t), (7.67, t), (7.9, d), (8.23, d), (8.34, s), (8.89, d), (8.76, d). ^{13}C CP MAS NMR (100.62 MHz, CDCl_3): δ = 131.1, 131.4, 132.2, 132.8, 135.1, 135.4, 137.4, 138.2, 147.2, 166.1, 166.5.

2.2.3. LDH/Ti(IV)-complex

One gram of Zn-Al/LDH was used after drying under reduced pressure at 100 °C. Thirty milliliter of ethanol was added to 1 g

dried LDH and stirred for 1 h. To an ethanolic suspension of LDH, 0.5 mmol (0.274 g) of metal complex was transferred and refluxed at 60 °C for 24 h with constant stirring. The final product was isolated by filtration, washed with ethanol and kept overnight in vacuum at 70 °C. The schematic representation of the total synthesis pathway is depicted in Scheme 1. Anal. Found/calcd(%). For $[\text{Zn}_2\text{Al}(\text{OH})_6\text{NO}_3](\text{Ti-complex})_{0.33} \cdot 0.63\text{H}_2\text{O}$ (Zn, Al-LDH/Ti-complex): Zn, 24.76/25.15; Al, 4.91/5.19; C, 16.48/16.75; N, 6.92/7.10; H, 2.08/2.28. IR (KBr) 3450, 3300, 1725, 1640, 1384, 675, 445 cm^{-1} .

Elemental analysis of LDH/Ti(IV)-complex gave 9.2 wt.% Ti. Hence, the uptake of metal complex is in the same proportion as the amount of Ti present. The ratio of Ti/Zn + Al in the final product is found to be 0.3.

2.3. Physico-chemical characterization of the catalyst

Powder XRD measurements were performed on a Rigaku D/MAX2500 diffractometer, using $\text{Cu K}\alpha$ radiation at 40 kV, 30 mA, a scanning rate of 5 °/min and a 2θ angle ranging from 3° to 80°. The FT-IR spectra of the samples were recorded using a Varian 800-FT-IR in KBr matrix in the range of 4000–400 cm^{-1} . The coordination environments of the samples were examined by diffuse reflectance UV-Vis spectroscopy. The spectra were recorded in a Varian-100 spectrophotometer in the wavelength range of 200–800 nm in BaSO_4 phase. Surface area was determined by N_2 adsorption-desorption at liquid nitrogen temperature (77 K) using ASAP 2020 (Micromeritics). Prior to adsorption-desorption measurement, the samples were equilibrated by degassing at 120 °C for 6 h. SEM images were obtained using HITACHI 3400N microscope. Thermogravimetric/differential thermal analysis (TG/DTA) was performed under air with a Shimadzu TGA-50 system at a heating rate of 5 °C min^{-1} . The chemical composition of the products was confirmed quantitatively and qualitatively by energy-dispersive X-ray (EDX) using a HITACHI 3400N microscope. The Ti loading in the catalyst and in the leaching solution was determined by using atomic absorption spectroscopy (Perkin-Elmer AAS 300 with acetylene (C_2H_2) flame). ^1H and ^{13}C CP MAS NMR spectra were recorded on 200 and 100.62 MHz, respectively, using a Bruker Avance 400 MHz spectrometer.

2.4. Catalytic reaction

Catalytic test of the prepared catalyst was carried out in a 100-ml two-necked round-bottom flask fitted with a reflux condenser. In a solvent-free condition, 10 mmol of cyclohexene and 0.05 g of catalyst were taken. To this, 30% H_2O_2 (30 mmol) was added dropwise. Reaction was carried out at 70 °C for 6 h (Scheme 2). The reaction products were analyzed by offline GC (Shimadzu GC-2010) equipped with a capillary column (ZB-1, 30 m length, 0.53 mm I.D. and 3.0 μ film thickness) using a flame ionization detector (FID). The selectivity of the epoxide (cyclohexene oxide) is a measure of the reactivity of the catalyst. The percentage of conversion of the substrate and the percentage of selectivity of the products in the epoxidation reaction are calculated as:

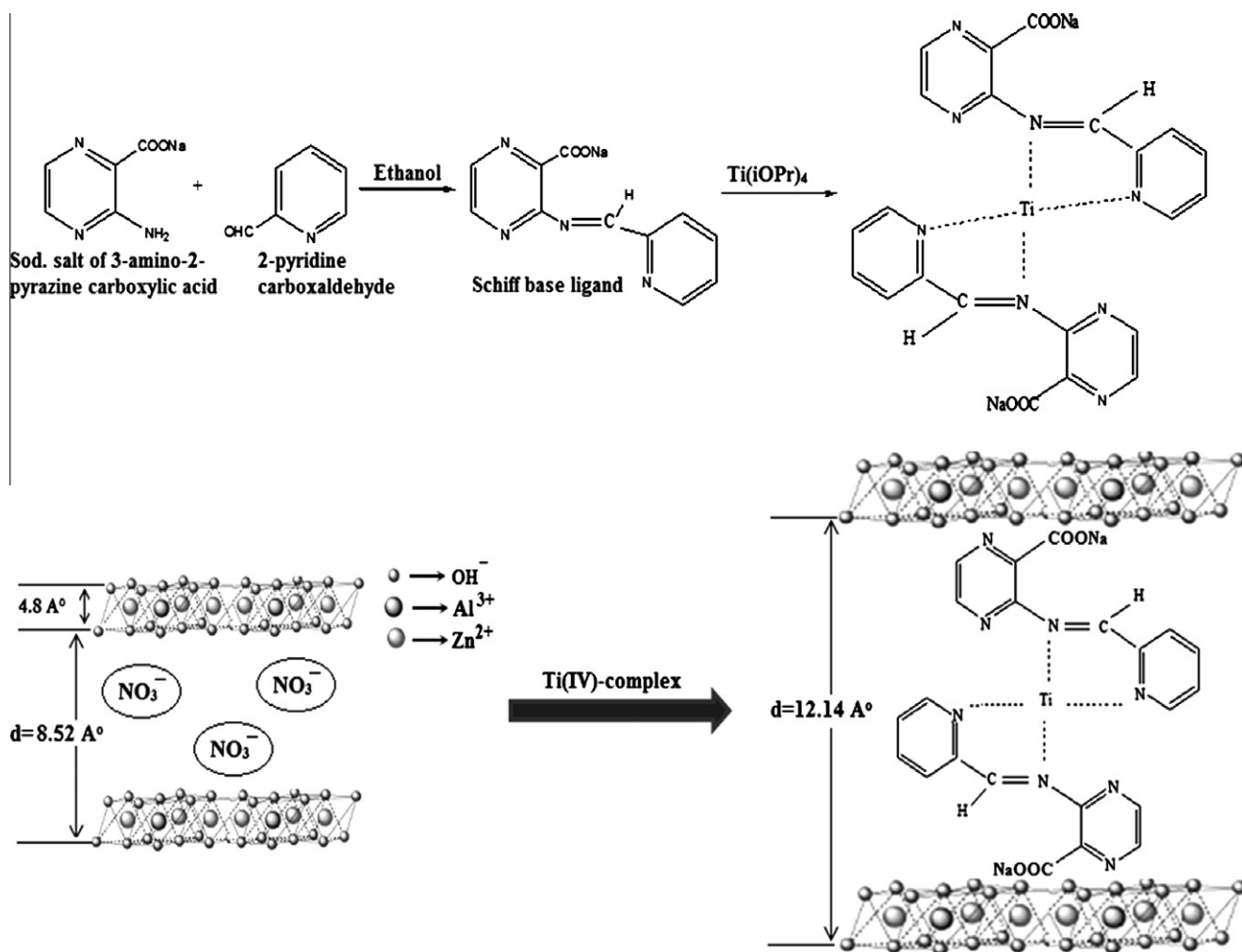
Substrate conversion (%)

$$= [\text{substrate converted (moles)}/\text{substrate used (moles)}] \times 100$$

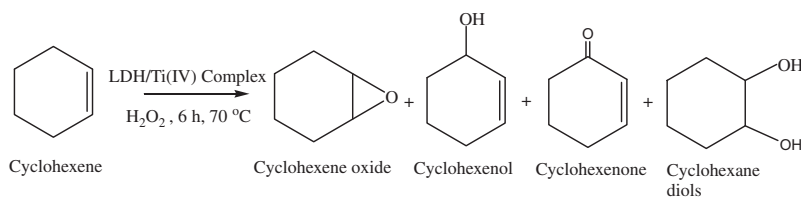
Product selectivity (%)

$$= [\text{product formed (moles)}/\text{substrate converted (moles)}] \times 100$$

The decomposition of H_2O_2 was followed by measuring the volume of oxygen liberated at atmospheric pressure by conventional gasometric method [28].



Scheme 1. Preparation pathway for the formation of LDH/Ti(IV)-complex.



Scheme 2. Catalytic reaction pathway.

Self-decomposition (SD) of H_2O_2

= volume of oxygen released in the reaction.

Conversion of H_2O_2

= consumption of H_2O_2 (including self-decomposition)
/initial amount of H_2O_2 .

3. Results and discussion

3.1. Catalyst characterization results

3.1.1. X-ray diffraction (XRD)

Fig. 1 shows the powder XRD patterns of (a) LDH (b) LDH/Ti(IV)-complex, (c) recycle catalyst (Fig. inserted). Zn–Al/LDH shows the

characteristic reflection for (0 0 3) plane at lower 2θ angle which corresponds to hydroxide layers. The basal spacing can be estimated from $d(0\ 0\ 3)$ position using Bragg's law, which is 8.52 Å [29]. The values obtained are in good agreement with the literature [30]. The intercalation of Ti(IV)–Schiff base complex has led to an increase in the basal spacing from $d = 8.52$ to 12.14 Å, where gallery height (7.34 Å) is calculated by subtracting brucite layer width (4.8 Å) [31] from basal spacing ($d = 12.14$ Å) as shown in Scheme 1 [32]. The increase in the basal distance confirms the intercalation of the complex anion. In case of complex-intercalated LDH, the $d(0\ 0\ 3)$ plane slightly shifted towards lower 2θ value. Again, the position of (1 1 0) reflection peak around $2\theta = 60^\circ$ after intercalation of the Ti-complex preserve indicates that the structure of the layer has been retained [33]. These sharp and symmetric peaks demonstrate the formation of a single well-crystallized Zn–Al/LDH. All the above results lead to conclude an easy intercalation process

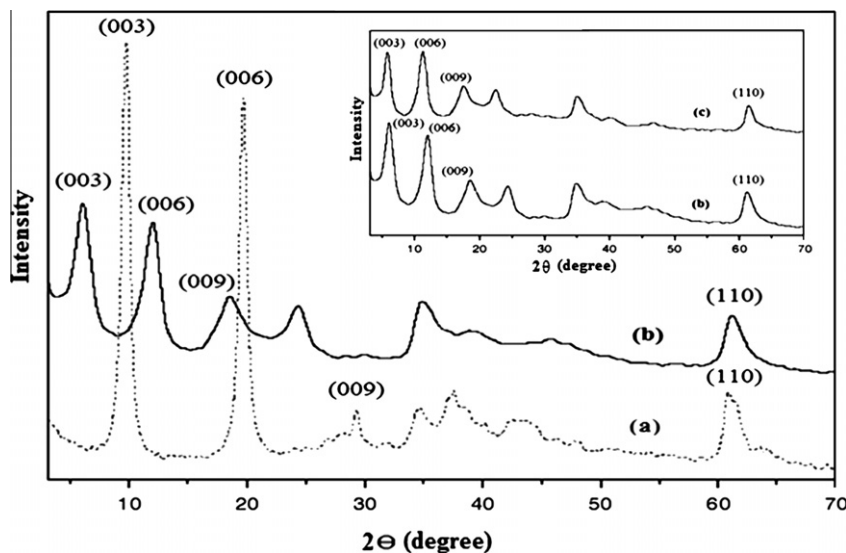


Fig. 1. XRD patterns of (a) LDH, (b) LDH/Ti(IV)-complex, and (c) recycle catalyst (inserted).

where the Zn–Al/LDH was prepared in an inert atmosphere [34]. In case of recycled catalyst (Fig. 1C inserted), all the peaks are retained in their respective position with respect to LDH/Ti(IV)-complex, suggesting properties of recycled catalyst remain unaltered.

3.1.2. FT-IR spectroscopy

The co-ordination environment around Ti and the process of intercalation can be investigated using FT-IR spectroscopy. The FT-IR spectra of (a) LDH, (b) Schiff base ligand, (c) Ti-complex, (d) LDH/Ti(IV)-complex and (e) recovered catalyst are shown in Fig. 2. The broad (as a result of hydrogen bonding) absorption in both spectra between 3600 and 3300 cm^{-1} is due to the $\nu(\text{OH})$ mode of the hydroxyl groups, both from the brucite-like layers and from interlayer water molecules. Interlayer water also gives rise to medium-intensity absorption close to 1620 cm^{-1} $\delta(\text{H}_2\text{O})$ [35]. The band at 1384 cm^{-1} is assigned to the stretching vibration of interlayer NO_3^- . The bands around 445 and 675 cm^{-1} are due to

Al–O and Zn–O lattice vibrations, respectively. Bands in the regions of 1640 and 1725 cm^{-1} are due to C=N stretching of imine and C=O stretching of carboxylate group. All the vibrations do not change significantly (Fig. 2e) compared to LDH/Ti(IV)-complex which suggests the existence of all the properties in the recycled catalyst.

3.1.3. UV-Vis spectral studies

The DRUV-Vis spectra of (a) LDH (b) Schiff base ligand (c) Ti(IV)-complex (d) LDH/Ti(IV)-complex are shown in Fig. 3. Bands around 250 nm is due to the benzenoid $\pi-\pi^*$ transition [36]. In case of Ti–Schiff base complex and LDH/Ti(IV)-complex, bands around 320 nm may be due to ligand-to-metal charge-transfer transition. Broad absorption band above 400 nm emerge in the spectrum can be attributed to the typical electronic transition of the aromatic ring and $-\text{C}=\text{N}$ conjugation ($n-\pi^*$ transition) system in a Schiff base and metal complex.

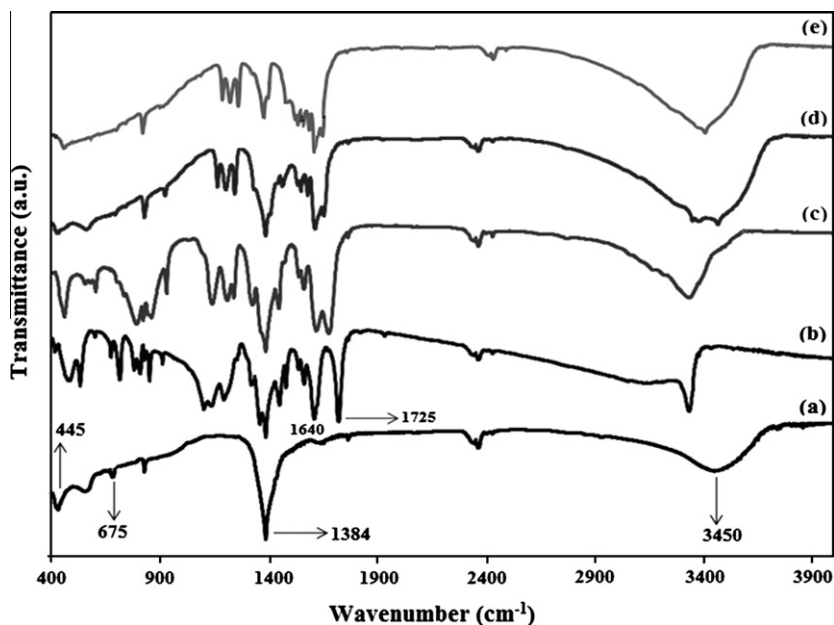


Fig. 2. FT-IR spectra of (a) LDH, (b) Schiff base ligand, (c) Ti(IV)-complex, (d) LDH/Ti(IV)-complex, and (e) recovered catalyst.

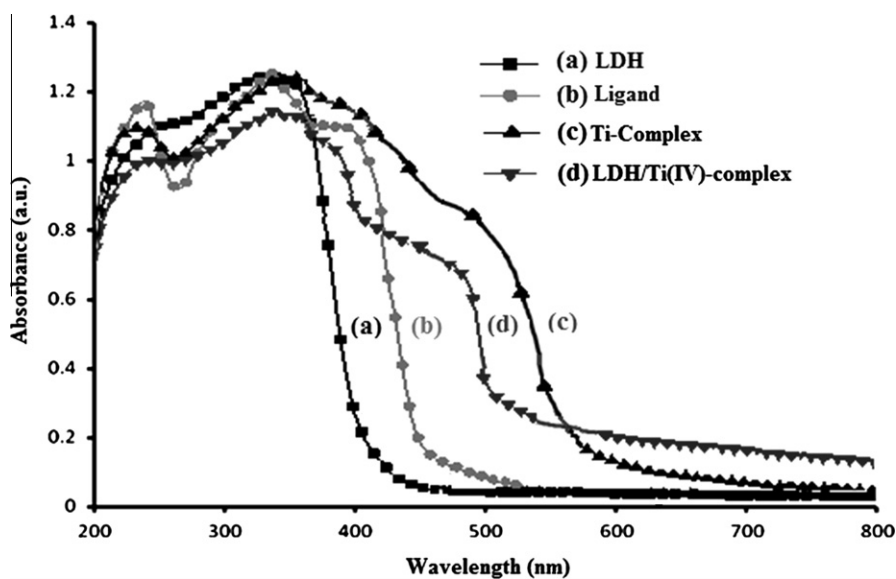


Fig. 3. Diffuse reflectance UV-Vis spectra of (a) LDH, (b) Schiff base ligand, (c) Ti(IV)-complex, and (d) LDH/Ti(IV)-complex.

3.1.4. N_2 adsorption-desorption studies

N_2 adsorption-desorption isotherms at 77 K for LDH and LDH/Ti(IV)-complex are shown in Fig. 4. Both the isotherms are of type II with a broad H3 type hysteresis loop [37]. Though isotherms for both the solids are quite similar, there is an increase in surface area for complex-intercalated LDH. The reason is that when bigger complex molecules are incorporated into the LDH layers, expansion takes place (i.e. increase in basal spacing from 8.52 to 12.14 Å). As a consequence, surface area of LDH/Ti(IV)-complex increases from 84 to 134 m^2/g .

3.1.5. Scanning electron microscope studies

The SEM images of Zn-Al/LDH and LDH/Ti(IV)-complex are shown in Fig. 5. Zn-Al/LDH presents discrete hexagonal plate-like morphology with sharp edges which indicate the formation of well-ordered LDH. In case of LDH/Ti(IV)-complex, some agglomerations are also observed due to the modification of LDH surface by metal complex intercalation [17].

3.1.6. TG/DTA analysis

The results of the thermal analysis of the materials are presented in Fig. 6. Generally, four steps are observed in the thermal

evolution of LDH [38] such as desorption of physically adsorbed water, removal of the interlayer structural water, dehydroxylation of the brucite-like sheets and the decomposition of the interlayer anions, although the first two steps may overlap in the low temperature range i.e. at 30–200 °C. The first two steps correspond to the removal of physically adsorbed and intergallery water (30–180 °C) and dehydroxylation of the brucite-like layers (180–290 °C). The third weight loss (290–550 °C) is due to decomposition of the interlayer nitrate anions [39]. There are three endothermic peaks in the DTA curve of ZnAl-NO₃/LDH (Fig 6a) appearing at 141, 232 and a sharp peak at 256 °C, respectively.

Incorporation of Ti-complexes, which are much larger than the nitrate anions, leads to a significant expansion of the interlayer spacing which in turn creates greater voids between the sheets and may facilitate the elimination of the interlayer water [40]. In the present case, the carbonyl oxygen atoms of coordinated carboxylate groups of Ti-complex are able to form a strong hydrogen bond which enhances the thermal stability of the hydroxyl layers. The higher thermal stability of the LDH/Ti(IV)-complex compared to Zn-Al/LDH can also be attributed to the higher charge density and larger number of COO⁻ groups in LDH/Ti(IV)-complex, which lead to stronger hydrogen bonding and other electrostatic interactions between the host and guest species [41]. For the LDH/Ti(IV)-complex (Fig. 6b), the thermal decomposition clearly proceeds in three distinct steps similar to LDH. The first one (30–300 °C, 14.8% mass loss) corresponds to the removal of coordinated water. The sharp mass loss observed in the range 300–400 °C (21.1%) is due to combustion of the organic ligand, with a corresponding sharp exothermic peak at 392 °C in the DTA curve. There is a third sharp mass-loss step in the range 400–600 °C (10.1%).

3.2. Catalytic reaction pathway

3.2.1. Catalytic performance in the epoxidation reaction

Epoxidation of olefins using different transition metal complex-supported mesoporous hosts and zeolites has been widely studied. The efficacy of homogeneous salen-based catalyst in olefin epoxidation was reported by Jacobsen et al. [42] and Irie et al. [43] in the early 1990s. These lead to an extensive effort in the design of their heterogeneous analogs using porous solid as a matrix [44–46]. Ballesteros et al. studied epoxidation of cyclohexene over different titanium alkoxo complexes immobilized on MCM-41,

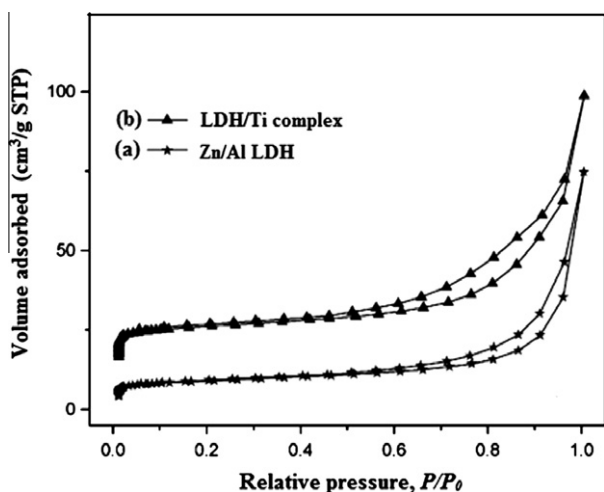


Fig. 4. N_2 adsorption-desorption isotherms of (a) LDH and (b) LDH/Ti(IV)-complex.

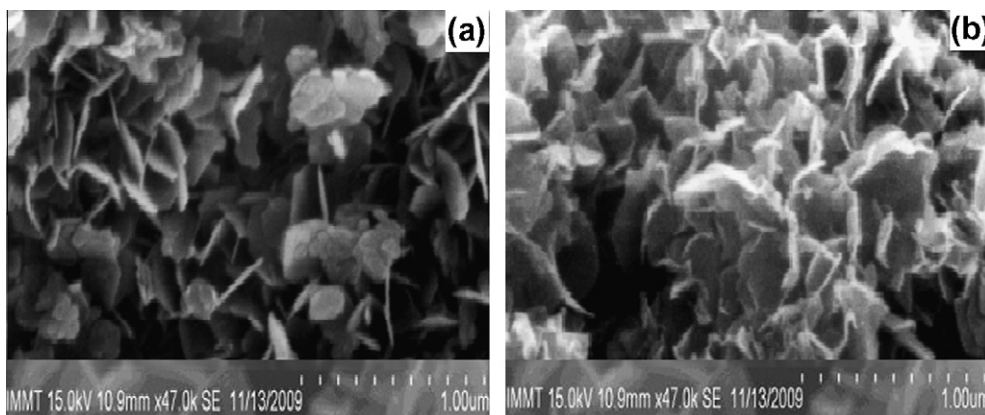


Fig. 5. SEM images of (a) LDH and (b) LDH/Ti(IV)-complex.

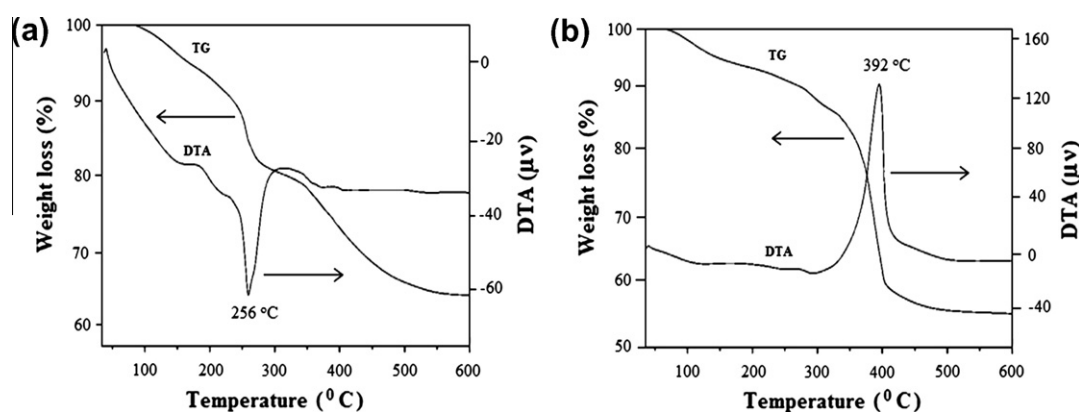


Fig. 6. TG/DTA curves of (a) Zn-Al/LDH and (b) LDH/Ti(IV)-complex.

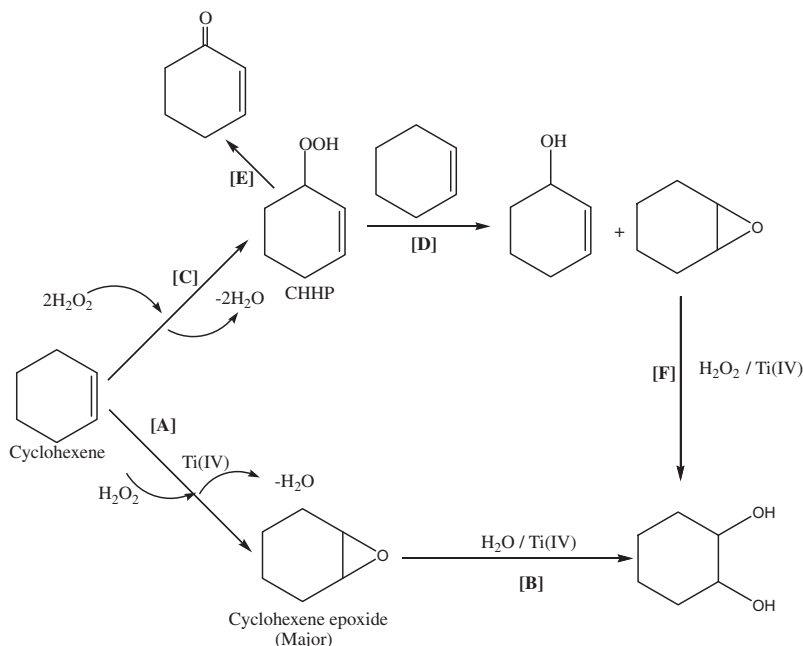
which showed up to 84% conversion using tert. butyl hydroperoxide (TBHP) as oxidant and dodecane as solvent at 60 °C in 24 h [47]. Berube et al. have reported an epoxidation catalyst based on Ti(acac)-complex immobilized on SBA-15, where they observed 43% conversion using TBHP as oxidant. This decrease in conversion may be due to blocking of pores, which partially deactivates the catalyst [48]. However, reports on epoxidation reactions over metal complex-intercalated LDH are rather limited. Bhattacharjee et al. have reported comparison of olefin epoxidation over different sulfonato-salen transition metal complex-intercalated LDH host with a maximum 83% conversion using molecular oxygen as oxidant in toluene medium [49]. It has been found in the present studies that 95% conversion took place with 84% selectivity towards epoxide in solvent-free condition (Table 1).

Using LDH/Ti(IV)-complex, the product is mostly cyclohexene epoxide accompanied by cyclohexenol, cyclohexenone and cyclohexane diol (Scheme 3). However, the catalytic epoxidation with H₂O₂ is usually a complicated process due to co-occurrence of several reactions. Our reaction is supposed to proceed via two types of mechanism, i.e. radical and nonradical pathway. Dropwise addition of H₂O₂ favors the nonradical pathway that increases the selectivity for epoxide [50]. In our proposed mechanism, in addition to direct epoxidation with hydrogen peroxide (path A), at least three more reactions took place. Another (path C) leads to the formation of allylic hydroperoxide, which can be used as oxidants for another epoxidation reaction with generation of epoxides and allylic alcohols (path D). Heterogeneous Ti(IV)-H₂O₂ system provides a better alternative for the production of epoxide. Addition of H₂O₂ to the titanium complex yields an oxygen-donating intermediate for

Table 1
Epoxidation of cyclohexene by different catalyst.

Catalyst	Conversion (%)	Epoxide selectivity (%)	Reference
Ti(IV)-Schiff base complex	62	79	This work
LDH/Ti(IV)-complex	95	84	This work
LDH-[Co(Cl)L]	83	64	[49]
Ti-HMDS-MCM-41	84	100	[47]

epoxidation reaction. It is generally agreed that the active intermediate is a titanium hydroperoxo species (Ti-OOH) opposed to a titanium peroxy species (Ti-OO) [51,52]. Regarding the mechanism of oxygen transfer in our system, a tentative explanation is an initial complex formation between metal catalyst (LDH/Ti(IV)-complex) and hydrogen peroxide which makes the peroxidic oxygen more electrophilic and labile to attack by an olefinic double bond [53]. Pathway C follows radical mechanism, where some of the H₂O₂ initially added was used. These radicals generate from the decomposition of peroxotitanium species by the reaction of H₂O₂ with titanium. Generation of cyclohexylene hydroperoxide (CHHP) is responsible for the formation of cyclohexenol, cyclohexenone and cyclohexane diol. The possibility to explain an increased selectivity of cyclohexenone is to suppose that it is formed by the decomposition of CHHP in the high injector temperature of the chromatograph (CHHP decomposes above 80 °C). The increase selectivity of cyclohexenone may presumably be due to further oxidation of cyclohexenol with time [54]. The plausible



Scheme 3. Plausible mechanistic pathway for cyclohexene conversion.

mechanistic path is shown in [Scheme 4](#). The effective utilization of H_2O_2 was found to be 91% (for 84% epoxide selectivity). Moreover, the epoxide suffers hydrolysis due to the presence of water-forming diol (path B in [Scheme 3](#)) with further increase in reaction time. The effect of reaction time on conversion and product selectivity is presented in [Table 2](#).

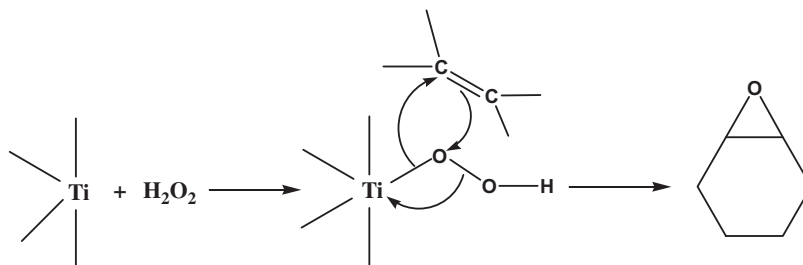
We have also tested our reaction using homogeneous Ti(IV)–Schiff base complex as catalyst, but it shows 62% conversion with 79% selectivity towards epoxide. In case of homogeneous complex, we get lower conversion when compared to its heterogeneous counterpart. This may presumably be due to the formation of catalytically inactive μ -oxo dimer by the homogeneous metal Schiff base complex. For example, the iron(III) porphyrins and phthalocyanines under oxidizing reaction conditions form dimeric forms containing LFe-O-FeL linkages (where L is a macrocyclic ligand), and in this form, they are unable to bind and activate oxygen. The possibility of increasing the catalytic life and possible enhancement of the rate of reaction lies in the ability to site isolate the catalyst on the support [55]. Hence, in case of LDH/Ti(IV)–complex, the active centers are well isolated and separated from each other, which facilitates the epoxidation reaction. Temperature has an enormous effect on conversion and selectivity of cyclohexene epoxidation. When the reaction was carried out at higher temperature i.e. around 80°C or above, the selectivity for cyclohexenone increases compared to cyclohexenol due to decomposition of CHHP. A combination of supported catalysts under solvent-free

condition can be used to carry out the epoxidation reaction in shorter time period with high conversion and selectivity [56]. The enhancement of rate may be attributed to the effect of dilution, i.e. the concentration of reactant is higher under solvent-free condition. However, on changing from homogeneous to heterogeneous phase, a slight increase in reaction time is observed under identical conditions. This is a general effect that arises upon immobilization of the metal complexes which imposes diffusion constraints on substrates and reactants by the layered structure [57].

In case of the present catalytic system, the conversion of epoxidation reaction depends on the amount of H_2O_2 added to the reaction medium. To evaluate this effect, we have monitored the progress of cyclohexene epoxidation in different molar ratios of oxidant and substrate ([Fig. 7](#)). It is found that at lower concentrations of oxidant, the conversion rate is very less, and with a gradual increase in oxidant amount, the conversion becomes higher. The optimum amount of H_2O_2 needed to achieve maximum conversion is 3:1 (oxidant/substrate). A further increase in molar ratio does not improve reaction conversion, but selectivity towards epoxide becomes less.

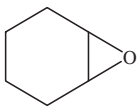
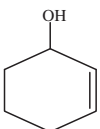
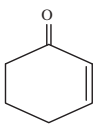
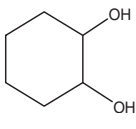
3.2.2. Heterogeneity test

Reutilization is one of the greatest advantages of heterogeneous catalyst, which can also provide useful information about intercalation process and catalytic stability along the catalytic cycles. To address the issue, a series of tests were undertaken. To test if metal



Scheme 4. Possible mechanism for the formation of epoxide.

Table 2
Effect of time on conversion of cyclohexene.^a

Time (h)	Conversion (%)	Selectivity (%)			
					
4	82	83	13	4	0
6	95	84	9	7	0
8	92	80	7	9	4
10	90	77	6	10	7

^a Reaction conditions: temperature 70 °C, H₂O₂ as oxidant, solvent-free condition.

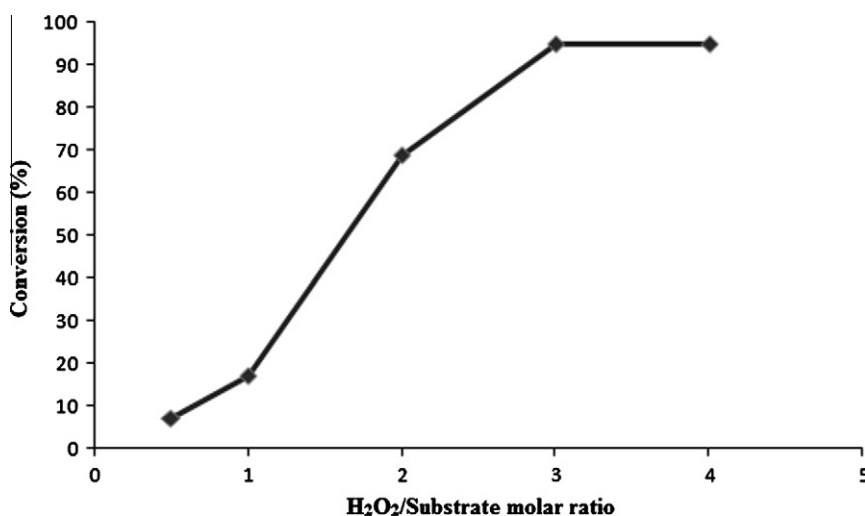


Fig. 7. Effect of H₂O₂ on conversion of cyclohexene.

Table 3
Recyclability test up to 3 cycles.^a

No. of cycles	Conversion (%)
1	95
2	92
3	87
4	84

^a Reaction conditions: temperature 70 °C, H₂O₂ as oxidant, solvent-free condition.

is leached out from the solid catalyst during reaction, the liquid phase of the reaction mixture is collected by filtration at the reaction temperature (70 °C). Atomic absorption spectrometric analysis of the liquid phase of the reaction mixtures thus collected by filtration confirms the absence of metal ions in the liquid phase. These experiments clearly demonstrate that metal does not leach out from the solid catalyst during epoxidation reaction. After the catalytic reaction were completed, solid catalyst was recovered by filtration and washed with ethanol several times and dried in open air. The recovered catalyst was then subjected to XRD, FT-IR spectroscopy. Comparison of XRD patterns and IR spectra of LDH/Ti(IV)-complex and recovered catalyst convincingly demonstrate that the structural integrity of the complex-intercalated LDH remains unaltered after the epoxidation reaction. Notably, the recovered catalyst can be reused in epoxidation reactions several times without appreciable loss of activity (Table 3)

4. Conclusions

In summary, it has been demonstrated that the LDH/Ti(IV)-Schiff base complex has a great potential for the environmentally benign epoxidation of cyclohexene with aqueous hydrogen peroxide under mild and organic solvent-free conditions. The catalyst was well characterized and confirms that there is a strong interaction between the host layers and intercalated organic anions. The proposed catalytic method is found to be an efficient pathway as a green alternative since it involves solvent-free condition. The stability of the catalyst has also been demonstrated convincingly by conducting three successive runs without appreciable loss of reactivity.

Acknowledgment

The authors are extremely thankful to Prof. B.K. Mishra, Director, IMMT, Bhubaneswar 751 013, Orissa, India, for his constant encouragement and permission to publish the paper.

References

- [1] J.M. DeSimone, *Science* 297 (2002) 799.
- [2] S.J. Jeon, H.M. Li, P.J. Walsh, *J. Am. Chem. Soc.* 127 (2005) 16416.
- [3] C.W. Jones, *Applications of Hydrogen Peroxide and Derivatives*, MPG Books Ltd., Cornwall, UK, 1999, 79.
- [4] K.A. Jorgensen, *Chem. Rev.* 89 (1989) 431.
- [5] S. Warwel, M. Rusch gen. Klaas, in: W. Adam (Ed.), *Peroxide Chemistry – Mechanistic and Preparative Aspects of Oxygen Transfer*, Wiley-VCH, Weinheim, 2000, p. 209.

- [6] W.R. Sanderson, *Pure Appl. Chem.* 72 (2000) 1289.
- [7] B.S. Lane, K. Burgess, *Chem. Rev.* 103 (2003) 2457.
- [8] T. Katsuki, K.B. Sharpless, *J. Am. Chem. Soc.* 113 (1991) 7063.
- [9] R.A. Sheldon, in: R. Ugo (Ed.), *Aspects of Homogeneous Catalysis*, vol. 4, D. Reidel, Dordrecht, 1981, p. 3.
- [10] R.A. Sheldon, J.A. Kochi, *Metal-Catalyzed Oxidation of Organic Compounds*, Academic Press, New York, 1981.
- [11] R.A. Sheldon, *Recl. Trav. Chim. Pays-Bas* 92 (1973) 253.
- [12] R.A. Sheldon, J.A. van Doorn, *J. Catal.* 31 (1973) 427.
- [13] R.A. Sheldon, *J. Mol. Catal.* 7 (1980) 107.
- [14] K.B. Sharpless, T.R. Verhoeven, *Aldrichim. Acta* 12 (1979) 63.
- [15] E. Klemm, E. Dietzsch, T. Schwarz, T. Kruppa, A.L. deOliveira, F. Becker, G. arkowz, S. Schirrmeister, R. Schutte, K.J. Caspary, F. Schuth, D. Honicke, *Ind. Eng. Chem. Res.* 47 (2008) 2086.
- [16] J.W. Johnson, in: M.S. Whittingham, A.J. Jacobson (Eds.), *Intercalation Chemistry*, Academic Press, New York, 1982, p. 267.
- [17] S.P. Newman, W. Jones, *New J. Chem.* 22 (1998) 105.
- [18] S. Carlino, *Solid State Ionics* 98 (1997) 73.
- [19] P.K. Dutta, D.S. Robins, *Langmuir* 10 (1994) 1851.
- [20] E. Klumpp, C.C. Ortega, P. Klahre, F.J. Tino, S. Yapar, C. Portillo, S. Stegen, F. Queirolo, M. Schwuger, *J. Colloids Surf. A* 230 (2003) 111.
- [21] H. Zhao, K.L. Nagy, *J. Colloid Interface Sci.* 274 (2004) 613.
- [22] F. Wypych, G.A. Bubniak, M. Halma, S. Nakagaki, *J. Colloid Interface Sci.* 264 (2003) 203.
- [23] S. Gago, M. Pillinger, A.A. Valente, T.M. Santos, J. Rocha, I.S. Goncalves, *Inorg. Chem.* 43 (2004) 5422.
- [24] K.A. Tarasov, D. O' Hare, V.P. Isupov, *Inorg. Chem.* 42 (2003) 1919.
- [25] L. Mohanambe, S. Vasudevan, *J. Phys. Chem. B* 109 (2005) 22523.
- [26] P. Tang, X. Xu, Y. Lin, D. Li, *Ind. Eng. Chem. Res.* 47 (2008) 2478.
- [27] Y.H. Chuang, Y.M. Tzou, M.K. Wang, C.H. Liu, P.N. Chiang, *Ind. Eng. Chem. Res.* 47 (2008) 3813.
- [28] S.B. Kanungo, K.M. Parida, B.R. Sant, *Electrochim. Acta* 26 (1981) 1157.
- [29] D. Carriazo, C. Martín, V. Rives, *Eur. J. Inorg. Chem.* 22 (2006) 4608.
- [30] S. Velu, V. Ramkumar, A. Narayanan, C.S. Swamy, *J. Mater. Sci.* 32 (1997) 957.
- [31] M.A. Drezdson, *Inorg. Chem.* 27 (1988) 4628.
- [32] R. Rhomer, J.E. Guerschais, *Bull. Soc. Chim. Fr.* (1961) 324.
- [33] G.R. Williams, D. O'Hare, *J. Mater. Chem.* 16 (2006) 3065.
- [34] J. Palomeque, F. Figueras, G. Gelbard, *Appl. Catal. A: Gen.* 300 (2006) 100.
- [35] C. Barriga, W. Jones, P. Malet, V. Rives, M.A. Ulibarri, *Inorg. Chem.* 37 (1998) 1812.
- [36] C. Hu, W. Zhang, Y. Xu, H. Zhu, X. Ren, C. Lu, Q. Meng, H. Wang, *Transit. Metal Chem.* 26 (2001) 700.
- [37] F. Rouquerol, J. Rouquerol, K. Sing, *Adsorption by Powders and Porous Solids: Principles Methodology and Applications*, Academic Press, San Diego, 1999, p. 439.
- [38] V. Rives, *Layered Double Hydroxides: Present and Future*, Nova Science Publishers, New York, 2001, p. 139.
- [39] S. Gago, M. Pillinger, T.M. Santos, J. Rocha, I.S. Goncalves, *Eur. J. Inorg. Chem.* 7 (2004) 1389.
- [40] F. Malherbe, J.P. Besse, *J. Solid State Chem.* 155 (2000) 332.
- [41] C. Li, L. Wang, D.G. Evans, X. Duan, *Ind. Eng. Chem. Res.* 48 (2009) 2162.
- [42] E.N. Jacobsen, W. Zhang, A.R. Muci, J.R. Ecker, L. Dent, *J. Am. Chem. Soc.* 113 (1991) 7063.
- [43] R. Irie, K. Noda, Y. Ito, N. Matsumoto, T. Katsuki, *Tetrahedron: Asymmetry* 2 (1991) 481.
- [44] C. Li, *Catal. Rev.* 46 (2004) 419.
- [45] C. Li, H. Zhang, D. Jiang, Q. Yang, *Chem. Commun.* (2007) 547.
- [46] C. Balezao, H. Garcia, *Chem. Rev.* 106 (2006) 3987.
- [47] R. Ballesteros, Y. Pérez, M. Fajardo, I. Sierra, I. del Hierro, *Micropor. Mesopor. Mater.* 116 (2008) 452.
- [48] F. Berube, B. Nohair, F. Kleitz, S. Kaliaguine, *Chem. Mater.* 22 (2010) 1988.
- [49] S. Bhattacharjee, T.J. Dines, J.A. Anderson, *J. Phys. Chem. C* 112 (2008) 14124.
- [50] E. Jorda, A. Tuel, R. Teissier, J. Kervennal, *J. Catal.* 175 (1998) 93.
- [51] M.G. Clerici, P. Ingallina, *J. Catal.* 140 (1993) 71.
- [52] W. Lin, H. Frei, *J. Am. Chem. Soc.* 124 (2002) 9292.
- [53] S. Khare, S. Shrivastava, *J. Mol. Catal. A: Chem.* 217 (2004) 51.
- [54] K.M. Jinka, J. Sebastian, R.V. Jasra, *J. Mol. Catal. A: Chem.* 274 (2007) 33.
- [55] T.J. Pinnavaia, E.M. Perez-Bernali, M. Chibwe, *US Patent No.* 5414080.
- [56] R.S. Varma, *Green Chem.* 1 (1999) 43.
- [57] B. Jarrais, A.R. Silva, C. Freire, *Eur. J. Inorg. Chem.* 22 (2005) 4582.